Research Square

Preprints are preliminary reports that have not undergone peer review.
They should not be considered conclusive, used to inform clinical practice,
or referenced by the media as validated information.

Geochemistry and physicochemical conditions of epsomite formation at Lece Mine (Southern Serbia)

Bratislav Todorovic

vinarce2001@yahoo.com

University of Niš

Tanja Petrović Pantić

Geological Survey of Serbia

Branko Matović

Vinča Institute of Nuclear Sciences

Marija Prekajski Đorđević

Vinča Institute of Nuclear Sciences

Nataša Radosavljević Stevanović

The National Forensic Centre

Amer Juma

University of Niš

Sandra Konstantinović

University of Niš

Research Article

Keywords: geochemistry, physicochemical, epsomite, Lece Mine

Posted Date: November 25th, 2026

DOI: https://doi.org/10.21203/rs.3.rs-10294777/v1

License: This work is licensed under a Creative Commons Attribution 4.0 International License.
Read Full License

Additional Declarations: No competing interests reported.

Geochemistry and physicochemical conditions of epsomite formation at Lece Mine (Southern Serbia)

Bratislav Todorović[1*], Tanja Petrović Pantić[2], Branko Matović[3]. Marija Prekajski Đorđević[3], Nataša Radosavljević-Stevanović[4], Amer Juma[1], Sandra Konstantinović[1]

[1]Faculty of Technology, University of Niš, Bulevar Oslobodjenja 124, 16000 Leskovac, Serbia

[2]Geological Survey of Serbia, Rovinjska 12, Belgrade, Serbia

[3]Vinca Institute of Nuclear Science, University of Belgrade, P.O. Box 522, 11001 Belgrade, Serbia

[4]The National Forensic Centre, Ministry of Interior of the Republic of Serbia, Belgrade, Serbia

***To whom all correspondence should be sent, e-mail: vinarce2001@yahoo.com**

Abstract Investigating the side effects and formation conditions of secondary minerals during the exploitation of underground mines is of great importance. This importance arises from the increasing demand for natural minerals/materials as well as from the need for preventive control of minerals that may pose health risks to miners. In this context, geochemical study were carried out to understand the formation of epsomite in the Lece Mine. FTIR analysis of the sample confirmed the presence of the mineral epsomite and revealed an "ice-like" water structure within the sample. This technique also explains the stretching and bending vibrations of the SO_4^{2-} anion. Asymmetric stretching vibrations were observed at 1103 and 1005 cm^{-1} (ν_3 and ν_1 modes) of SO_4^{2-}, while the band at 628 cm^{-1} corresponds to bending vibrations (ν_4). In addition, FTIR analysis indicates the presence of metal-O (in this case Mg–O bonds). XRD and SEM-EDS analyses further confirmed the presence of pure fibrous epsomite. The fibers have lengths of 6–8 cm and diameters ranging from 6–12 μm. Particularly interesting results were obtained from the investigation of the mineral base supporting epsomite formation. These studies revealed the presence of two minerals significant for its formation: meixnerite and birnessite. Meixnerite acts as a precursor of Mg^{2+} cations, whereas birnessite provides sufficient MnO_2, which catalytically promotes the oxidation of S_2^{2-}/S^{2-} to SO_4^{2-}. These ions originate from the large number of sulfide minerals present in the mine, mainly FeS_2. The presence of these precursors, together with the evaporation of ground waters (relative air humidity > 90%), explains the formation of epsomite. This is further supported by investigations of the physicochemical formation conditions, which indicate a relatively low temperature range (287–289 K), Eh ≥ 0.25 V, and formation in a slightly acidic to neutral environment (pH ≤ 7).

Key words geochemistry, physicochemical, epsomite, Lece Mine

Acknowledgments

This research is a part of the Project 451-03-34/2026-03/200133 supported by the Ministry of Science, Technological Development and Innovation of the Republic of Serbia and the Faculty of Technology in Leskovac.

Introduction

Epsomite ($MgSO_4 \times 7H_2O$) is a mineral that is commonly found in marine evaporite deposits, saline lakes, and within the zones of metal and coal mines (Stober et al. 2023). Interestingly, it has also been identified in chondritic meteorites and icy satellites (Frederiksson and Kerridge 1988). The mineral has an orthorhombic structure, a hardness of 2-2.5 (Mohs), and represents a water structure maker (Jini et al. 2023). This conclusion is further supported from a macroscopic standpoint by viscosity measurements. Epsomite is widely distributed worldwide, with the largest and most famous deposits located in the USA, Spain, the Czech Republic, Italy, and Russia. On the Balkan Peninsula, it has been discovered in mines in Bulgaria, Greece, Romania, North Macedonia, and Serbia (Badovac-Gračanica).

The structure of epsomite has been extensively studied and has been known since 1964 (Baur 1964). The mineral consists of $Mg(H_2O)_6^{2+}$ octahedra and SO_4^{2-} tetrahedra, while the seventh water molecule is not directly bonded to magnesium but occupies the voids within the crystal lattice. Studies on the stability of compounds of the type $MgSO_4 \times nH_2O$ have shown that epsomite is stable at temperatures <298 K, while at temperatures >298 K it loses one water molecule from its structure (e.g., at 298-311 K it transforms into $MgSO4 \times 6H_2O$; Ruiz-Agudo et al, 2007; Ruiz-Agudo et al, 2007). Conversely, Fortes et al. (2006) indicated that this mineral can persist at temperatures up to 320 K, depending on the concentration of $MgSO_4$ (>32 %).

In the present case, this mineral was identified in the Lece Mine, at depths of 110 m and 130 m. This mine is primarily known for the exploitation of lead and zinc ores. Among the nonmetallic minerals, various carbonates, sulfides, quartz, and apatite are the most abundant. Since no free sulfur was detected, the precursor of the SO_4^{2-} anion in epsomite could only originate from the oxidation of S_2^{2-}/S^{2-} anions. The oxidation of these species is well documented in aqueous solutions and marine sediments (Zehnder and Schoch 2009).

From an industrial perspective, epsomite is used for the production of Epsom salts, which are applied in the paper, sugar, and pharmaceutical industries. It is also added to bath water to reduce stress and relieve pain. This mineral is particularly appreciated by gardeners, as it promotes better flowering of plants. In addition to the aforementioned uses, epsomite is most commonly applied as a fertilizer, and more recently as a material for energy storage (Gurevich et al. 2007; Meril, 2021). This property is attributed to its high density and the ability to undergo reversible hydration/dehydration (Iype et al. 2018; Sato and Hattanji 2018). In the ceramic industry, its use is associated with mass loss and temperature variation studies. However, in practice, a wider application of this mineral is limited by its slow kinetics and structural transformations (Zhang et al. 2014).

Geological setings

The mine is located in southern Serbia, about 40 km from the city of Leskovac. The Lece andesite Massif, also known as the Lece Volcanic Complex, covers an area of over 700 km². The Lece ore deposit (lead, zinc, and silver) is situated on the eastern margin of the massif.Volcanic activity began during the Upper Oligocene and continued throughout the Miocene. It was initiated by the effusive phase of amphibolic andesite, followed by explosive volcanism that produced large accumulations of pyroclastic rocks, including volcanic breccias, agglomerates, and tuffs.

Subsequent eruptions generated new andesitic masses that solidified in shallow crustal levels.These volcanic rocks overlie crystalline schists, Cretaceous sediments, and Jurassic serpentinites.

Calderas (Fig. 1) with outpourings of dacite-andesite, pyroclastite and tuffs were formed in collapsed crystalline blocks. The quartz-breccia zones indicated the presence of a reactive type of caldera, along which intensive hydrothermal changes of the rocks took place. The multiphase nature of volcanic activity is confirmed by normally and reversely magnetized andesites as a product of the youngest phase of Tertiary magmatism (Vukašinović 2005). The magma intrusion formed a wide doma, which caused the characteristic semicircular shape of the river valleys.

Dominant rocks of the Lece volcanic complex are andesite, dacite, trachyte, and propylite, with a vast presence of pyroclastic rocks (Fig 2), formed during multiple phases of explosive eruptions. Andesites dominate in the central part of the massif, while pyroclastic sediments dominate in the peripheral parts. Two groups of andesites are distinguished: amphibolic and pyroxenitic. Amphibolic andesitesare presented by hornblende andesite, hornblende-pyroxene andesite, hornblende- pyroxene-biotite andesite, and transitional types to dacites. Pyroxene andesites represent younger members of the volcanic complex. Dominant minerals in these rocks are augit and hyperstene (Pešut 1976). After volcanic activity, a tectonic movement created structures such as fractures, dislocations and faults. The main structurewithin which the deposit Lece was formed extends in the direction NNW-SSE. These structures were active in the past, resulting in the formation of mineral deposits within them. Mineral deposits are formed by the precipitation of minerals from hydrothermal fluids as a result of changes in temperature and pressure, typically under low-temperature and low-pressure conditions. Dominant ore minerals are sphalerite, markesite, pyrite, chalcopyrite, galenite, enargit, hematite, gold, antimonite…(Pešut 1976). Sulphides mainly have a lens shape. The secondary minerals in deposits are limonite, covelline, cerussite, anglesite, smithsonite, chalcanthite, and melanterite. A several km long zone of silicification, hydrothermal breccias, is a main carrier of a low-temperature metal ore complex, such as the deposits with increasing gold concentrations - the Majdan Lece mines (Stajević 2002). A large fault zone is a heat conductor for thermal water of Sijarinska Banja (Todorović et al, 2015) located south-eastern of Lece,while the thermal waters of Prolom Banja are topped by wells completed in the andesites on the massif itself (Petrović-Pantić 2015).

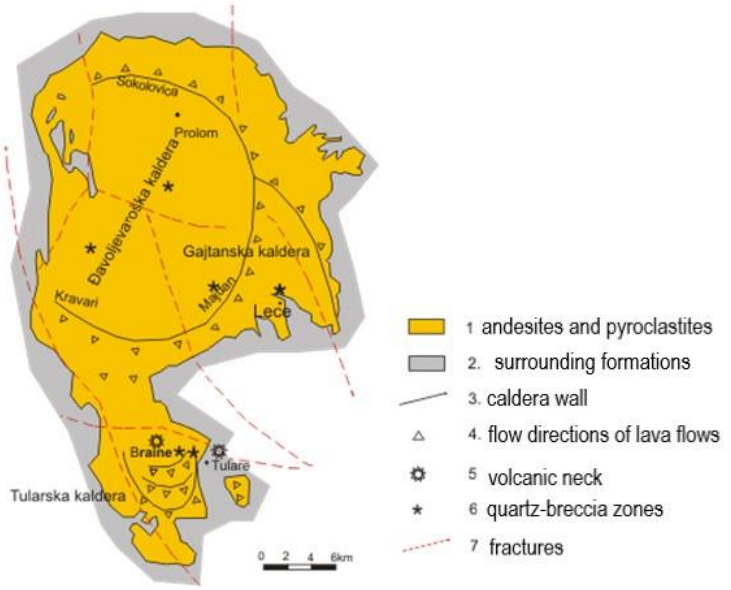

Fig. 1 Sheme of Lece volcanic complex (Jovanović et al 1972; Petrović 2010)

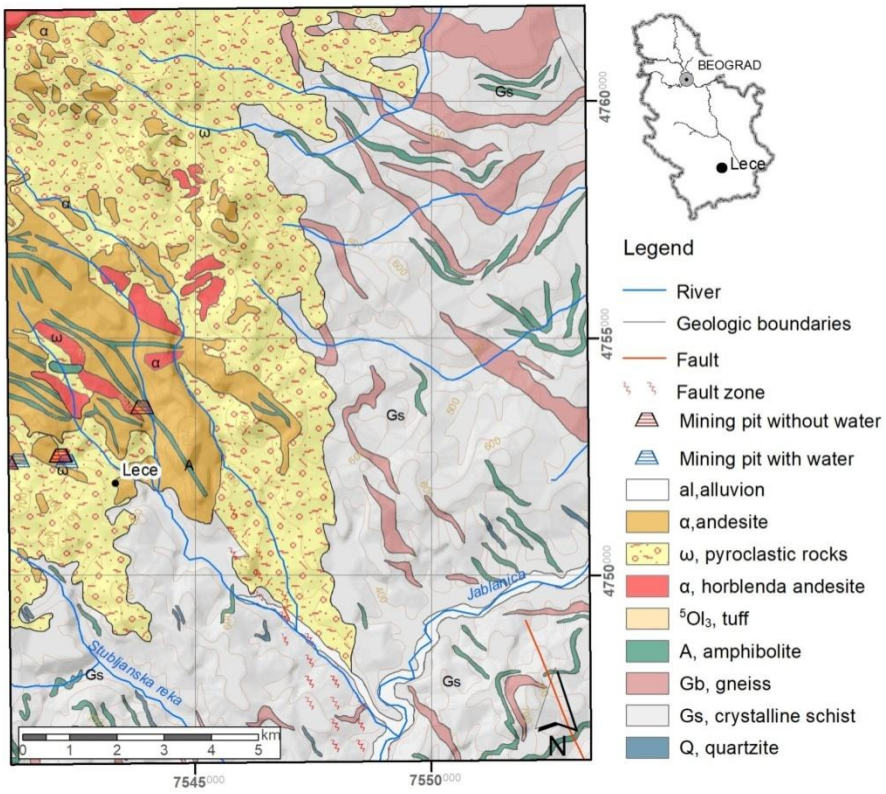

Fig. 2 Geological map of the Lece andesite massif (modified after Basic Geological Map of SFRY, 1:100,000, sheets Podujevo (Vukanović et al, 1980) and Leskovac (Dimitrijević et al, 1965)

Ekspertimental

During the hydrogeological investigations conducted for the preparation of the 1:100,000 Basic Hydrogeological Map, Leskovac Sheet, mineral samples were collected inside the Lece Mine in November 2019.

Fourier transformation infrared spectroscopy (FTIR). Recording of FTIR spectra was performed on a BOMEM Michelson Series MB FTIR spectrometer, in the range of 4000 to 400 cm^{-1}. The so-called "potassium bromide" solid sample preparation method was used for sample preparation. 0.5-2 mg of sample was mixed with 150 mg of spectroscopically pure KBr. The mixture was then subjected to vacuum and pressed under pressure, whereby the corresponding pellet was obtained. Spectroscopically pure KBr, manufactured by Merck, was previously melted at 973 K, ground and stored in an electric desiccator heated to 573 K, to eliminate moisture. A pellet of pure KBr was used as a reference pellet.

SEM-EDS analysis. Samples were recorded on a Fei S50 inspect scanning electron microscope with a tungsten filament. The samples were preliminarily imaged with a BSD detector at 25 keV, without coating, and at this stage elemental qualitative and quantitative analysis was also performed. After that, the samples were coated with C and observed with an ET-detector (SE) at a column voltage of 5 Kev and various magnifications, from 300 X to 30,000 X.

X-ray powder diffraction (XRD) analysis. This analysis was used for mineral identification of collected samples, using Raguku Ultima IV powder diffractometer. The X-ray beam was nickel-filtered $CuK\alpha_1$ radiation (λ = 0.1540 nm, operating at 40 kV and 40 mA). XRD data were collected from 5 to 90° (2θ) in a continuous scan mode with a scanning step size of 0.02° and at a scan rate of 5°/min. Phase analysis accompanied with Rietveld refinement was done by using the PDXL2 software (version 2.0.3.0) [23], with reference to the patterns of the International Centre for Diffraction Database (ICDD) [24], version 2012.

Results and discussion

Ftir analysis. The FTIR spectrum of the sample indicates the presence of a large amount of water, and unlike XRD, it provides information about its nature and structural organization. According to previous studies, the water in the analyzed sample may exist in both “ice-like” and “liquid-like” structural forms, depending on whether tetrahedral hydrogen bonding between water molecules is complete or incomplete (Cheng et al., 2013). A broad and intense band with multiple small peaks in the range of 3600-3200 cm^{-1} corresponds to the O–H stretching vibrations of water molecules (Fig. 3). This type of vibration also appears as a broad, low-intensity band with a small peak around cm^{-1}. The peaks observed at 3200–3350 cm^{-1} and 3450–3600 cm^{-1} correspond to clusters of crystallization water molecules, representing the “ice-like” water structure (Eisenberg and Kauzmann 1962; Ovalles et al. 2009; Cheng et al. 2013). The bending vibration of water haves peaks in the area at 1685-1630 cm^{-1}. The strong and sharp peak at 1103 cm^{-1} with shoulder at 1005 cm^{-1} are the asymmetric stretching vibration (ν3) and asymmetric stretching vibration (ν1) of SO_4^{2-}. The peak at 628 cm^{-1} is due to ν4 bending vibrations. The sharp peak at 422 cm^{-1} possibly are due to metal-O bonds (Mg-O).

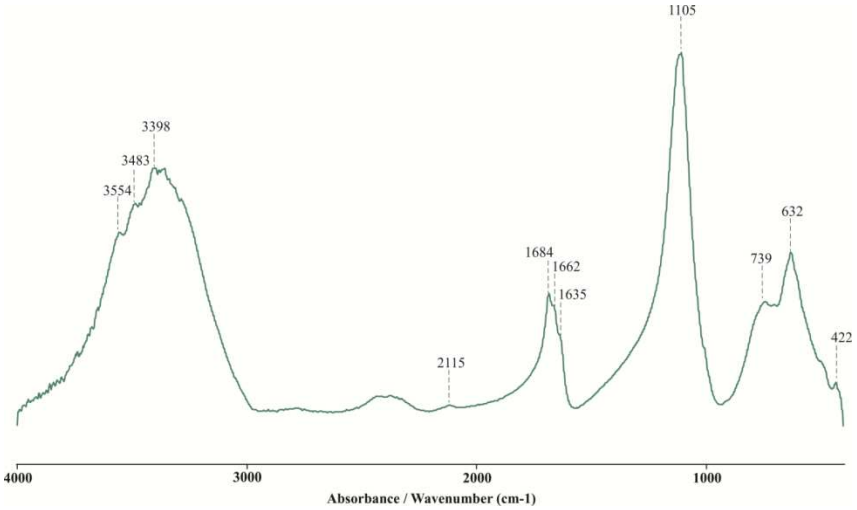

Fig. 3 FTIR spectrums of sample in the 2000-400 cm^{-1} region

SEM-EDS analysis. At the Lece mine, epsomite occurs on two levels, at depths of approximately 110 m and 130 m. The mineral appears as botryoidal masses composed of tiny fibrous to acicular transparent crystals, forming woolly efflorescence. It typically develops in the corners between the wall and the ceiling, forming deposits that resemble a spider web in appearance. A few days after sampling and removal from the mine, the fibers changed color, turning from transparent to white or grayish (Fig. 4). The SEM micrographs reveal a large number of fibers with lengths of 6–8 cm and diameters ranging from 6–12 μm, showing morphology characteristic of $MgSO_4$ phases (EDS spectrum, Fig. 5).

The EDS spectrum also indicates the presence of Mn_xO_y type compounds. This impurity originates from the base of the sample, which contains minor fragments of host rock. According to Aller and Rude (1988), Mn^{4+} cations are more favorable than other oxidation states of Mn during the oxidation of S_2^{2-}/S^{2-} to SO_4^{2-}, which may explain the occurrence of manganese oxides within the examined material.

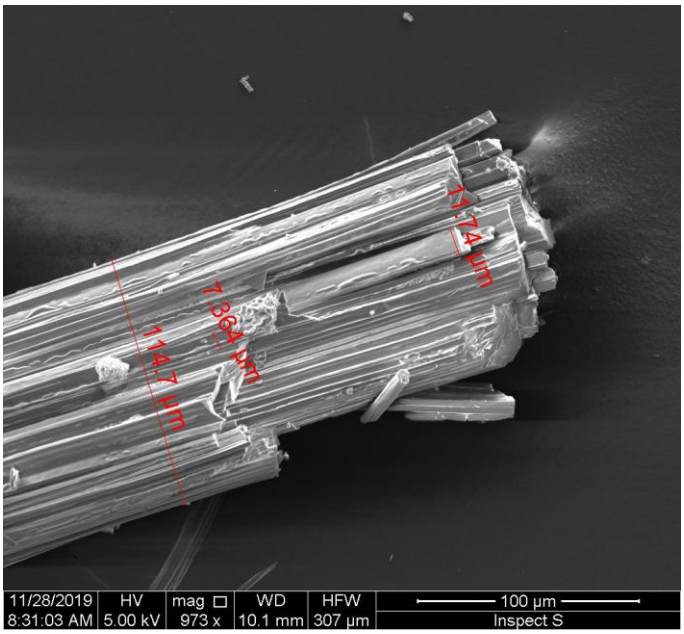

Fig. 4 SEM of epsomite

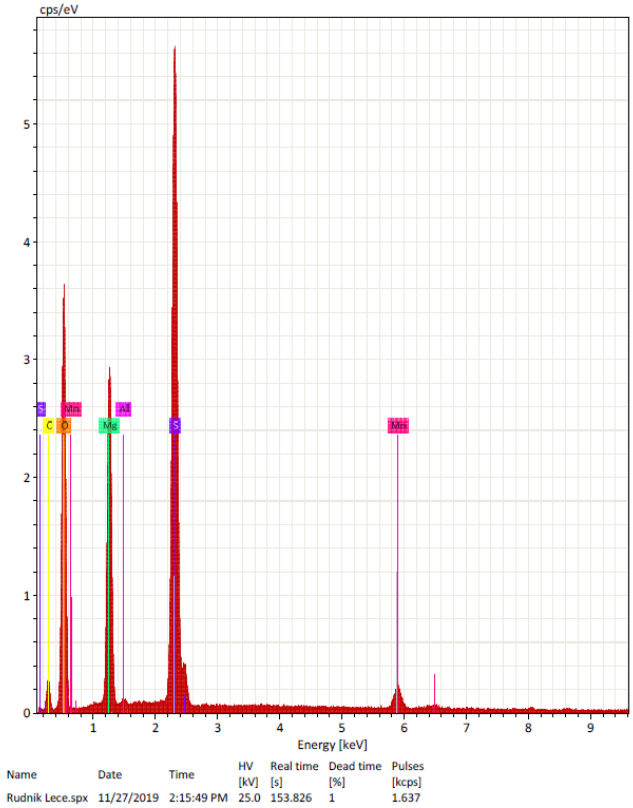

Fig. 5 EDS of epsomite

XRD analysis. This analysis confirmed that the sample composed of thin white needle-like crystals consists of pure epsomite (Card No. 01-072-0696; Fig. 6). In addition to the needle structures, the base of the sample was also

analyzed in order to determine the paragenesis and identify the associated minerals (Fig. 7). The results revealed the presence of two additional mineral phases: meixnerite [$Mg_6Al_2(OH)_{16}\times4H_2O$] (Card No. 00-050-1684) and birnessite ($Na_{0.55}\,Mn_2O_4\times1.5H_2O$; card No: 00-043-1456). Meixnerite is considered a probable precursor of Mg^{2+} cations in the formation of epsomite. The presence of Birnessite at the base of the needle aggregates explains the Mn signal observed in the EDS spectrum, since this mineral-through its catalytic properties-can facilitate the formation of SO_4^{2-} anions (Yücel et al. 2010, Avetisyan et al., 2021).

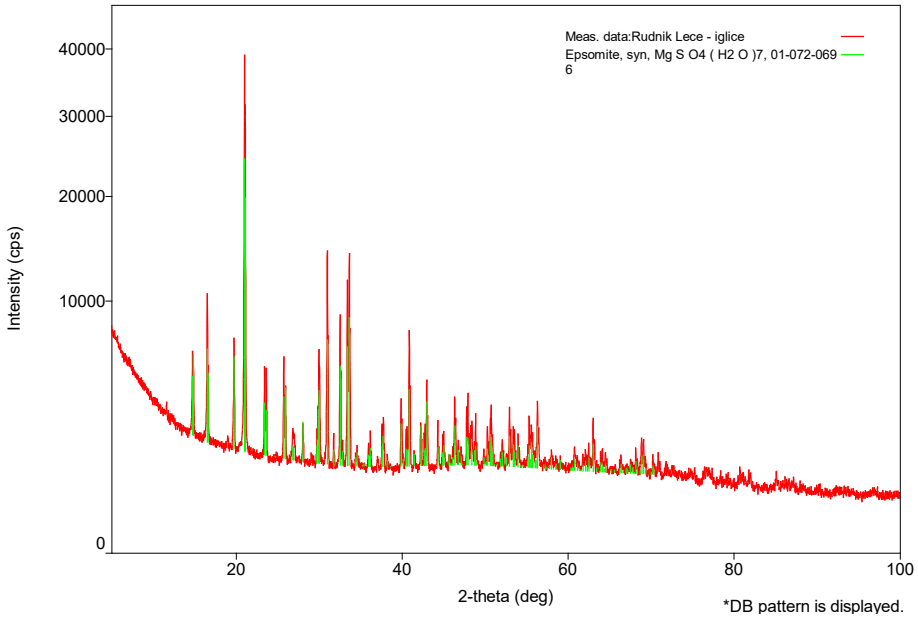

Fig. 6 XRD spectrum of epsomite

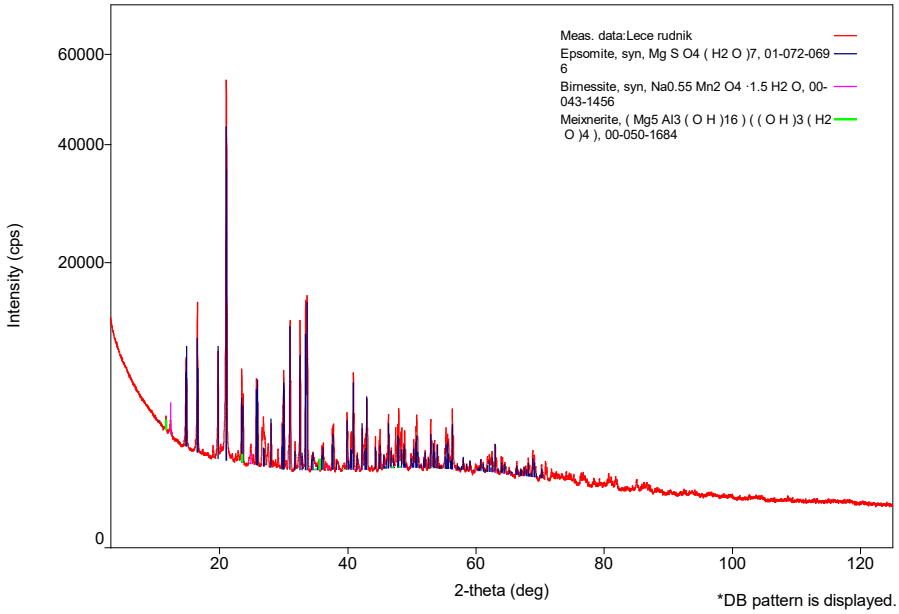

Fig. 7 XRD pattern of epsomite and associated admixtures at the base of the needle aggregates

Formation mechanism of epsomite and physicochemical conditions. The analyzed epsomite samples could not have formed by the deposition of sulfur and magnesium-rich water during mining operations, since no such precipitates were observed after the openings were made, and the samples were found high on the walls and ceilings. Because no sulfur-bearing compounds were detected at the base of the epsomite aggregates, the SO_4^{2-} anions likely originated from S_2^{2-}/S^{2-} anions. These anions are abundant in the Lece mine, where they occur as accompanying phases of lead and zinc ores (such as pyrite, sphalerite, enargite, galena, and chalcopyrite). Since pyrite (FeS_2) is the most abundant and widespread sulfide mineral in the ore, it was considered the primary precursor of SO_4^{2-} anions. It is well known that Fe^{2+} and Mn^{2+} ions enhance the oxidation of solid sulfide S^{2-} species (Vasquez et al., 1989; Poulton et al. 2004; Yücel et al. 2010). In this case, the oxidation kinetics of S_2^{2-}/S^{2-} and intermediate sulfur compounds are promoted by the presence of birnessite, which is a precursor of MnO_2. Acting as a catalyst, MnO_2 helps to overcome the kinetic barrier for the oxidation of S_2^{2-}/S^{2-} species by molecular oxygen (Konovalov et al., 2003; Luther et al., 2011). According to Schippers and Jørgensen (2001) and their subsequent studies, the oxidation of these anions to SO_4^{2-} may proceed via two pathways: the thiosulfate mechanism and the polysulfide mechanism. The presence of pyrite as the dominant sulfide mineral in the deposit supports the thiosulfate oxidation pathway, leading to the formation of S_2^{2-} anions (McNeice et al. 2022). Groundwater infiltration into the mine, which must be continuously pumped out, creates high humidity, providing a more than sufficient supply of H_2O molecules necessary for the crystallization of $MgSO_4{\times}7H_2O$ (Wildner et al. 2022). Accordingly, the following mechanism of epsomite formation is proposed:

$$FeS_2 + 7.5\ MnO_2 + 11\ H^+ \rightarrow Fe(OH)_3 + 2SO_4^{2-} + 7.5\ Mn^{2+} + 4H_2O \qquad (1)$$

$$Mg^{2+} + SO_4^{2-} + 7H_2O \rightarrow MgSO_4{\times}7H_2O \qquad (2)$$

The formation of epsomite most likely occurred on the rock surface, where Meixnerite acted as the precursor of Mg^{2+} cations and Birnessite as the precursor of MnO_2. The opening of mine workings inevitably led to an increase in the redox potential (Eh). According to Eh–pH diagrams for Mg^{2+} cations, there exists a wide thermodynamic field of stability for this ion at pH <11 (Fig. 8). Special attention was therefore given to the thermodynamic stability field of the FeS_2/SO_4^{2-} system, which defines the range of Eh–pH conditions under which the oxidation of S_2^{2-} to SO_4^{2-} anions is thermodynamically favored.

Based on these, S_2^{2-} anion exhibit a broad stability range under both oxidizing and reducing conditions, which overlaps with the stability domain of SO_4^{2-} at pH >1.5. During ore exploitation and the opening of new mine levels, the Eh increased, leading to the oxidation of S_2^{2-} to SO_4^{2-} (equation 1). Since no pyrite or other S_2^{2-}/S^{2-} phases were found at the base of the epsomite aggregates, it is evident that the Eh during epsomite formation was ≥0.25 v. Njegov raspad se je odigrao u skladu sa reakcijom (1), a Eh vrednost je verovatno bliska samoj granici (0.025; Fig. 8). In

addition to the elevated Eh, the high relative humidity of the air (90–91%) and the moderately low temperature range (287-289 K) represent favorable physicochemical conditions for the crystallization of epsomite (equation 2).

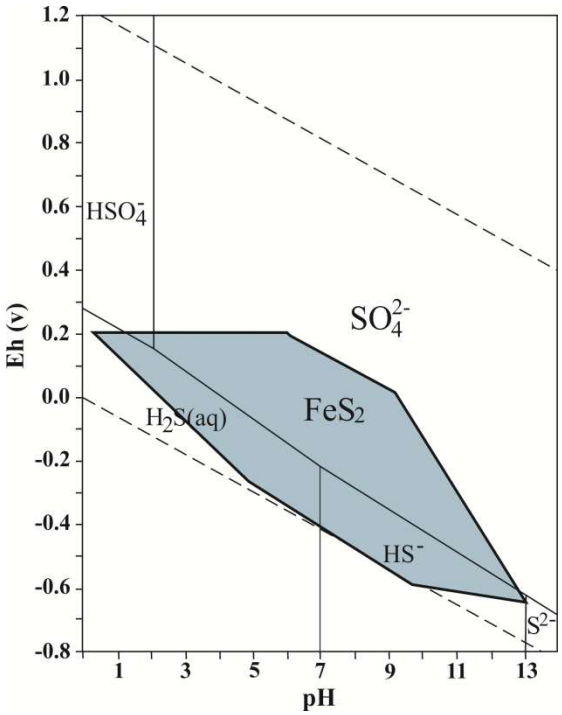

Fig. 8 Eh-pH diagram of pyrite and sulfur species (based on Takeno 2005)

The rate of S^{2-} oxidation to SO_4^{2-} can be described as a second-order reaction. The rate constant (K) depends on both temperature (T) and pH, and their interrelationship was defined by Igumnov (1976) and Ahmoto and Lasaga (1982). According to these authors, a decrease in pH (i.e., under more acidic conditions) leads to a reduction in the rate constant, with this trend being valid down to pH 3. At pH 4-7, the rate constant remains approximately constant, whereas at pH >7, it decreases again. Based on these observations, it is assumed that the oxidation of S_2^{2-} to SO_4^{2-} occurred under slightly acidic to neutral conditions (pH ≤7), at the Eh ≥ 0.25 V.

Conclusion

FTIR, SEM-EDS and FTIR techniques detect the sample as pure epsomite without the presence of admixtures. FTIR analysis of O-H detects water as an "ice-like" structure (multiple smaller peaks in the area 3600-3200 cm^{-1}). Also, this analysis shows asymmetric stretching vibration and bending vibration of SO_4^{2-}. The Asymmetric stretching vibration su na 1103 cm^{-1} (ν3) i 1005 cm^{-1} (ν1). The bending vibrations is peak at 628 cm^{-1} (ν4). The peak at 422 cm^{-1} possibly are due to Mg-O bonds. SEM-EDS and XRD techniques detect minerals at its base (meixnerite and birnessite). Underground water vapors and thus detected meixnerite in the mine can be considered the progenitor of the epsomite. The presence of birnessite catalytically aids the oxidation S_2^{2-}/S^{2-} to SO_4^{2-}. Physicochemical conditions for the crystallization of epsomite are Eh ≥0.25, pH ≤7, high relative humidity (90–91 %), temperature range (287-289 K).

Funding The authors declare that there is no specific funding for this project.

References:

Aller RC, Rude PD (1988) Complete oxidation of solid phase sulfides by manganese and bacteria in anoxic marine sediments. Geochim Cosmochim Acta. https://doi.org/10.1016/0016-7037(88)90335-3

Avetisyan K, Zweig I, Luther GW, KamyshnyA (2021) Kinetics and mechanism of polysulfides and elemental sulfur formation by a reaction between hydrogen sulfide and δ-MnO_2. Geochim Cosmochim Acta. https://doi.org/10.1016/j.gca.2021.08.022

Baur WH (1964) On the crystal chemistry of salt hydrates. IV. The refinement of the crystal structure of MgSO4.7H2O (epsomite). Acta Crystallogr https://doi.org/10.1107/S0365110X64003449

Dimitrijević MD, Petrović B, Čikin M, Možina A, Vukanović M, Karajičić Lj (1965) Basic geological map of the Republic of Serbia 1:100.000, sheet Leskovac, Savezni geološki zavod, Belgrade, https://geoliss.mre.gov.rs/prez/OGK/RasterSrbija/

Eisenberg D, Kauzmann W (1969) Structure and Properties of Water, Clarendon Press, Oxford.

Fredriksson K, Kerridge JF (1988) Carbonates and Sulfates in CI Chondrites: Formation by Aqueous Activity on the Parent Body. Meteoritics. https://doi.org/10.1111/j.1945-5100.1988.tb00894.x

Gavrichev KS. et al. (2007) Heat capacity and thermodynamic functions of epsomite MgSO4·7 H2O at 0–303 K. Geochem Int https://doi.org/10.1134/S0016702907020103

Gurevich VM, Kuskov OL, Cheng F, Cao Q, Guan Y, Cheng H, Wang X, Miller JD (2013) FTIR analysis of water structure and its influence on the flotation of arcanite (K_2SO_4) and epsomite ($MgSO_4 \cdot 7H_2O$), Int Journal Miner Process. https://doi.org/10.1016/j.minpro.2013.04.007

Igumnov SA, (1976) Sulfur isotope exchange between sulfide and sulphate in hydrothermal solutions, Geokhimiya, 4: 497-503.

Iype E, Khalfay ZSA, Chaudhuri RG, Kumar P, (2018) Epsomite dehydration: A molecular dynamics study, J Energy Storage. https://doi.org/10.1016/j.est.2018.10.005

Jini D, Aravind M, Alsaiari NS, Alzahrani, FM, Sillanpaa, M. (2023) Investigation on structural, optical, morphological, electrical, mechanical and biological activities of pure and crystal violet dye-doped epsomite single crystals. J Mater Sci. https://doi.org/10.1007/s10854-022-09468-z

Jovanović M, Karajičić, Lj, Karamata S, Vukanović M (1972) New Insights into the Evolution of Volcanism in the Lece Andesitic Complex, Geological Annals of the Balkan Peninsula, Vol. 37, Part 2 (pp. 165–177)

Konovalov SK,. Luther GW, Friederich GE, et al (2003) Lateral injection of oxygen with the Bosporus plume-fingers of oxidizing potential in the Black Sea. Limnol Oceanogr. https://doi.org/10.4319/lo.2003.48.6.2369

Luther GW, Findlay AJ, MacDonald DJ, Owings SM, Hanson TE, Beinart RA, Girguis PR (2011) Thermodynamics and Kinetics of Sulfide Oxidation by Oxygen: A Look at Inorganically Controlled Reactions and Biologically Mediated Processes in the Environment. Front Microbiol. https://doi.org/10.3389/fmicb.2011.00062

Merrill A (2021) Magnesium Compounds. United States Geological Survey-Mineral Commodity Summaries.

McNeice J, Mahandra H, Ghahreman A (2022) Biogenesis of thiosulfate in microorganisms and its applications for sustainable metal extraction. Rev Environ Sci Biotechnol. https://doi.org/10.1007/s11157-022-09630-3

Ohmoto H, Lasaga AC (1982) Kinetics of reactions between aqueous sulfates and sulfides in hydrothermal systems, Geochim Cosmochim Acta. https://doi.org/10.1016/0016-7037(82)90113-2

Ovalles F, Gallignani M, Rondón R, Brunetto MR, Luna R (2009) Determination of Sulphate for Measuring Magnesium Sulphate in Pharmaceuticals by Flow Analysis-Fourier Transforms Infrared Spectroscopy. Lat Am J Pharm 28: 173-82

Petrović Pantić T, Birke M, Petrović B, Nikolov J, Dragišić V, Živanović V (2015) Hydrogeochemistry of thermal groundwaters in the Serbian crystalline core region. J Geochem Exploration. https://doi.org/10.1016/j.gexplo.2015.08.009

Pešut, D. 1976. Geology, tectonics and metallogeny of Lece massif, Discussions of the Institute for Geological and Geophysical Research, XIV, Belgrade

Poulton S.W, Krom MD, Raiswell R (2004) A revised scheme for the reactivity of iron (oxyhydr)oxide minerals towards dissolved sulfide. Geochim Cosmochim Acta. https://doi.org/10.1016/j.gca.2004.03.012

Ruiz-Agudo E, Mees F, Jacobs P. et al. (2007) The role of saline solution properties on porous limestone salt weathering by magnesium and sodium sulfates. Environ Geol. https://doi.org/10.1007/s00254-006-0476-x

Ruiz-Agudo J, Martín-Ramos D, Rodriguez-Navarro Carlos (2007) Mechanism and Kinetics of Dehydration of Epsomite Crystals Formed in the Presence of Organic Additives. J Phys Chem B. https://doi.org/10.1021/jp064460b

Sato M, Hattanji TA (2018) A laboratory experiment on salt weathering by humidity change: salt damage induced by deliquescence and hydration Prog Earth Planet Sci. https: //doi.org/10.1186/s40645-018-0241-2

Schippers A, Jørgensen BB (2001) Oxidation of pyrite and iron sulfide by manganese dioxide in marine sediments. Geochim Cosmochim Acta. https://doi.org/10.1016/S0016-7037(00)00589-5

Stober I, Zhong J, Bucher K (2023) From freshwater inflows to salt lakes and salt deposits in the Qaidam Basin, W China. Swiss J Geosci. https://doi.org/10.1186/s00015-023-00433-4

Stajević B (2004) Geochemical haloes of gold in the Lece ore field (southern Serbia), Geol Anali Balk poluos. 65: 93-99

Takeno N (2005) Atlas of Eh–pH diagrams. Geological Society of Japan, Open File Report

Todorović B, Stojiljković D, Petrović Pantić T, Mitić N, Nikolić Lj, Cakić S (2015) Hydrogeochemistry and aragonite scaling in the Sijarinska spa (Serbia). Carbonates Evaporites https://doi.org/10.1007/s13146-015-0266-1

Vazquez FG, Zhang J, Millero FJ (1989) Effect of metals on the rate of the oxidation of H2S in seawater. Geophys. Res. Lett. https://doi.org/10.1029/GL016i012p01363

Vukanović M, Dimitrijević MD, Dimitrijević MN, Karajičić Lj, Rajčević D, Navala M, Urošević M, Malešević M, Trifunović S, Serdar, R, Atin B (1964-1975), Basic geological map of the Republic of Serbia 1:100.000, sheet Podujevo, Savezni geološki zavod, Belgrade https://geoliss.mre.gov.rs/prez/OGK/RasterSrbija/

Vukašinović S (2010) Presentation and interpretation of the aeromagnetic map of the Republic of Serbia 1:100.000. Geoinstitute, Belgrade.

Wildner M, Zakharov BA, Bogdanov NE, Talla D, Boldyreva EV, Miletich R (2022) Crystallography relevant to Mars and Galilean icy moons: crystal behavior of kieserite-type monohydrate sulfates at extraterrestrial conditions down to 15 K. IUCr. https://doi.org/10.1107/S2052252521012720

Yücel M, Konovalov SK, Moore TS, Janzen CP, Luther GW (2010) Sulfur speciation in the upper Black Sea sediments. Chem Geol. https://doi.org/10.1016/j.chemgeo.2009.10.010

Zehnder K, Schoch O (2009) Efflorescence of mirabilite, epsomite and gypsum traced by automated monitoring on-site J Cult Herit https://doi.org/10.1016/j.culher.2008.10.009

Zhang H, Iype E, Nedea SV, Rindt CCM (2014) Molecular dynamics study on thermal dehydration process of epsomite (MgSO4·7H2O). Mol Simul https://doi.org/10.1080/08927022.2013.854891